Journal of Polymer Research (2021) 28: 430
https://doi.org/10.1007/s10965-021-02803-8

ORIGINAL PAPER

Designed azo-linked conjugated microporous polymers for CO_2 uptake and removal applications

Ahmed F. Saber[1] · Kuan-Ying Chen[1] · Ahmed F. M. EL-Mahdy[1] · Shiao-Wei Kuo[1]

Received: 22 September 2021 / Accepted: 18 October 2021 / Published online: 23 October 2021

Abstract

In recent decade, conjugated microporous polymers (CMPs) were treated as one of the superior porous materials for CO_2 uptake. Herein, we prepared two azo-linked CMPs namely: azo-carbazole (Azo-Cz) and azo-phenothiazine (Azo-Tz) from the reduction of the corresponding nitro monomers using sodium borohydride ($NaBH_4$). The obtained polymers were well characterized using many spectroscopic techniques. According to TGA and BET analyses, our CMPs owned good specific surface areas (reaching 315 $m^2\ g^{-1}$), and a significant thermal stability. It is also possessed pore sizes of 0.79 and 1.18 nm, respectively, and a reasonable char yields (max. 46 %). Based on CO_2 uptake measurements, the CO_2 adsorption capacities of these CMPs were very good: up to 40 and 94 mg g^{-1} at the experiment temperatures 298 and 273 K, respectively. The great CO_2 uptake is due to high surface areas that facilitate powerful interactions with CO_2 molecules.

Keywords Azo-linked · Conjugated microporous polymers · CO_2 uptake · Surface area

Introduction

Carbon dioxide (CO_2) emission and its critical impacts such as global warming, sea level rising, and ocean acidity increasing were considered from the remarkable environmental issues [1–3]. CO_2 capturing and storage technology have garnered a considerable attention over the past two decades, due to increasing its level in atmosphere at an alarming rate which is currently recorded as 35 billion tons/year [4]. The master source of this abnormal elevation is attributed to fossil fuels that comprises about 85 % of all energy consumption [5, 6], as apparent from the sharp decline in the daily international CO_2 emission at the beginning of the year 2020 comparable to that of the previous year 2019, as a result of covid-19 situation that lockdown a great number of industries worldwide [7]. The first attempt for CO_2 capture was depend on liquid amine adsorption [8]. However, this strategy faced a lot of challenges including solvent loss, storage difficulty, corrosion nature, toxicity impact, instability at high temperature and high cost [9, 10]. Due to the above stated drawbacks, liquid amine method was replaced by other solid alternates containing pore network structures for CO_2 adsorption and separation via physisorption process. These porous solid materials have many advantages of depressed energy consuming, outstanding cycling ability, and facile regeneration [11–15]. Activated carbons, zeolites, conjugated polymers, metal organic frameworks (MOFs), covalent organic frameworks (COFs), and covalent triazine frameworks (CTFs) are few examples among the solid sorbents for gas uptaking and other potential applications [16–31]. The best example for this purpose was the versatile materials called microporous organic polymers (MOPs) which combining high surface areas, tunable pore sizes, high chemical stability with diverse synthetic procedures [32–36]. MOPs have successfully applied in numerous applications including energy storage, hydrogen evolution from water, dye removal from wastewater, gas adsorption, and chemosensing [32–38]. Therefore, such candidates have exhibited hopeful prospects in CO_2 uptake.

MOPs with tiny pore size (>2nm) are rated as hopeful materials for CO_2 removal strategies, due to the closeness of their pore sizes to the molecular dimensions of CO_2 and other small gases [39]. Conjugated microporous polymers (CMPs) are a recently sub-divided category of MOPs that features a lot of merits over

✉ Ahmed F. M. EL-Mahdy
ahmedelmahdy@mail.nsysu.edu.tw

✉ Shiao-Wei Kuo
kuosw@faculty.nsysu.edu.tw

[1] Department of Materials and Optoelectronic Science, Center of Crystal Research, National Sun Yat-Sen University, Kaohsiung 80424, Taiwan

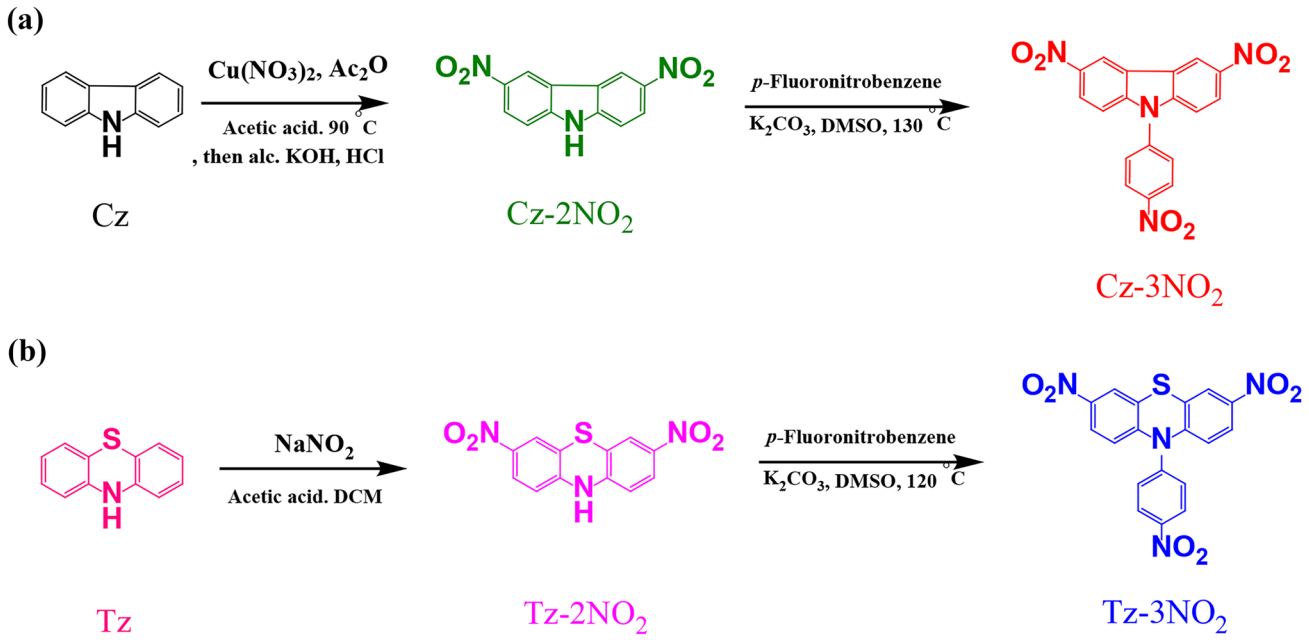

Scheme 1 Synthesis of (**a**) 3,6-dinitro-9-(4-nitrophenyl)carbazole (Cz-3NO_2) and (**b**) 3,7-dinitro-10-(4-nitrophenyl)-*10H*-phenothiazine (Tz-3NO_2)

other materials mentioned above, including molecular design flexibility, [40–44] inherent porosity, low structural density, surface area rising, tailorable surface properties and useful applications, such as gas storage and separation, [45, 46] supercapacitors, [47, 48] light emission, [49, 50] chemical sensing, [51, 52] and heterogeneous catalysis [53, 54]. Capturing and separation of CO_2 is considered one of the most studied applications of CMPs, [55–58] as they can be readily functionalized by the insertion of a particular CO_2-philic groups like rich-π moieties, acidic or basic units to promote CO_2 uptake and separation [59–62]. As an example, NPOF-4-NH_2, which were yielded from the nitro-electrophilic substitution of NPOF-4 followed by reduction of these nitro-groups, show high selectivity towards CO_2/N_2 (139 mol mol^{-1}) through Lewis acid-base interaction [63]. Moreover, some azo-linked porous polymers (ALPs) have been synthesized for CO_2 removal. For example, Arab et al. [64] prepared a group of new azo-bridged polymers, with a moderate BET surface area in the range of 412–801 m^2 g^{-1}, that displayed CO_2 adsorption capacities reached to 2.94 mmol g^{-1} at 298 K/1 bar with a good selectivity. Another reported work of ALPs that presented both higher surface area of 862–1235 m^2 g^{-1} and good CO_2 capture capacities of up to 5.37 mmol g^{-1} at 237 K/1 bar, have been synthesized by coupling of aniline-like molecules in the presence of copper(I) bromide and pyridine [65]. From these investigations, one can conclude that the porosity factors (surface area, pore size and pore volume) were from the major reasons affecting on CO_2 uptake capacity and selectivity.

Considering the above aspects, herein, we have designed and synthesized two azo-containing CMPs namely: azo-carbazole (Azo-Cz) and azo-phenothiazine (Azo-Tz), through one-pot reductive reaction of car-3NO_2 (Scheme 1a) and phenothiazine-3NO_2 (Scheme 1b) monomers with sodium borohydride ($NaBH_4$) under relatively mild synthetic conditions Scheme 2. We used a lot of techniques to elucidate their chemical structures, surface areas, pore size distributions, thermal stability, microporous structures and surface morphology such as Fourier transform infrared (FTIR) spectroscopy, solid state ^{13}C nuclear magnetic resonance (NMR) spectroscopy, the Brunauer–Emmett–Teller (BET) method, thermogravimetric analysis (TGA), scanning electron microscope (SEM) and transmittance electron microscope (TEM), respectively. These two CMPs possessed high porosity, large BET surface areas and moderate thermal stabilities. Interestingly, they also featured exceptional adsorption capacities toward carbon dioxide gas, achieving maximum uptake efficiency reaching to 40 and 94 mg g^{-1} at the experiment temperatures 298 and 273 K, respectively; a good value comparable with those of the best recently reported CMPs listed in Table 2.

Experimental section

Materials

All used solvents and chemicals were obtained from commercial suppliers and used as received unless otherwise noted. Carbazole, copper (II) nitrate trihydrate (98 %), acetic anhydride (99 %), acetic acid (99.8 %) were ordered

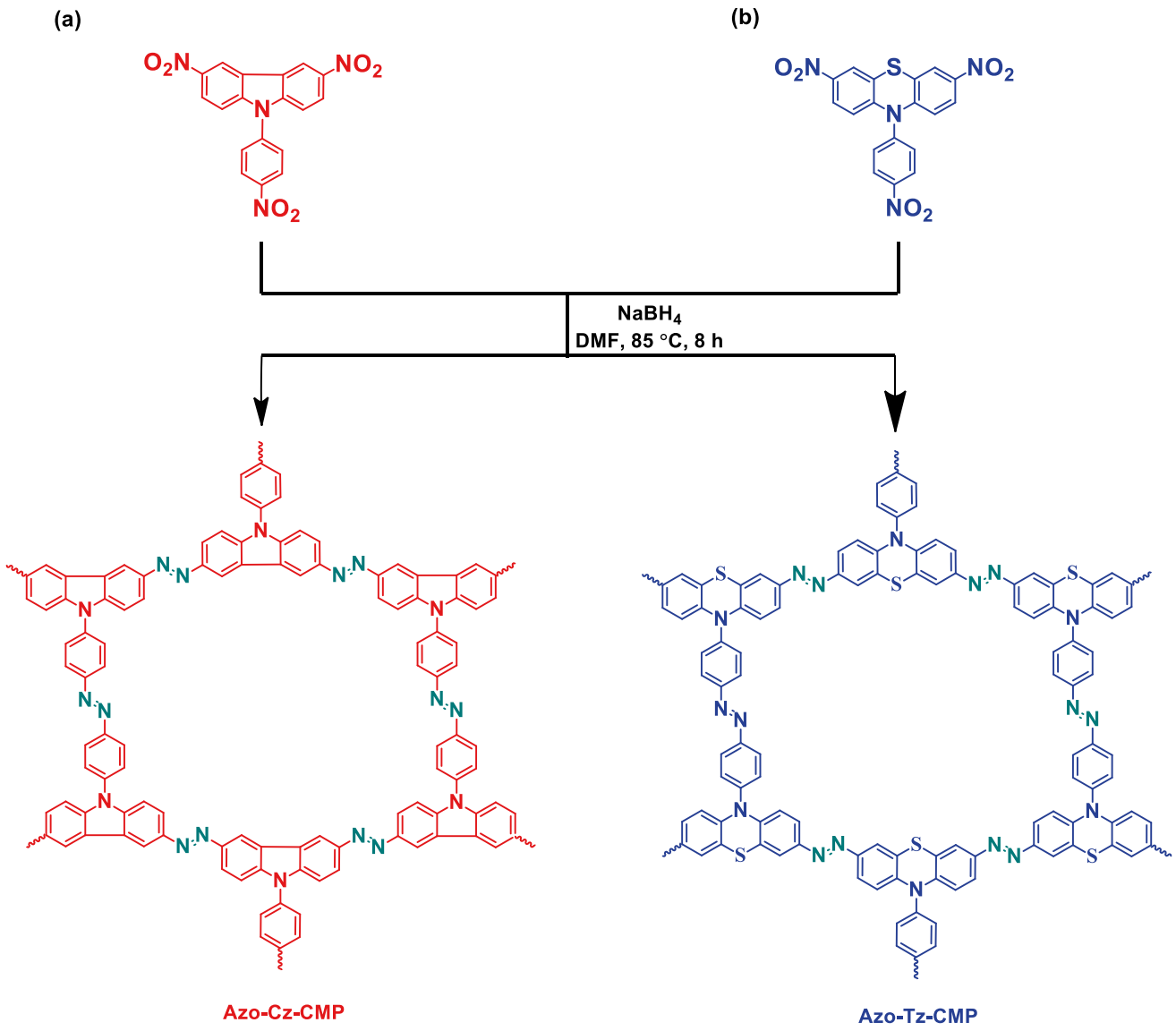

Scheme 2 Preparation of (**a**) Azo-Cz-CMP and (**b**) Azo-Tz-CMP

from Sigma. 1-Fluoro-4-nitrobenzene (99 %) and potassium carbonate (99%) were purchased from Alfa Aesar. Sodium borohydride ($NaBH_4$, 99%), phenothiazine, dimethylformamide (DMF) and dichloromethane (DCM) were purchased from J. T. Baker. Tetrahydrofuran (THF, 99.9%) was ordered from Showa (Tokyo, Japan), whereas ethanol was gained from ECHO chemical company, Taiwan.

Synthesis of 3,6-dinitro-9H-carbazole (Cz-2NO_2) [Scheme 1(a) and Scheme S1]

In a 250 mL two neck round-bottomed flask, $Cu(NO_3)_2.2.5H_2O$ (7.3 g, 30 mmol) was firstly dissolved in acetic anhydride/acetic acid mix (50 mL, 3:2 v/v) at room temperature. Carbazole (4.2 g, 25 mmol) was added progressively in small portions to this homogenous solution within 15 min at temperature of 15–20 °C. After that, the reaction temperature was allowed to warm to ambient temperature over a period of 30 min before heating to 90 °C for an extra 30 min. Finally, quenching of the reaction mixture into distilled water (250 mL) was carried out to produce the solid precipitate which was gathered by filtration, and further washed five times with distilled water (100 mL). The obtained precipitate (2.0 g) was dissolved in alcoholic potassium hydroxide solution (130 mL, 6% wt/v) to isolate 3,6-dinitro-*9H*-carbazole (Car-2NO_2) from the other formed isomeric dinitrocarbazoles. After stirring the above solution for 30 min at 50 °C, the insoluble portion was collected by filtration and washed three times with distilled water (20 mL). The alkaline alcoholic filtrate was neutralized with

concentrated hydrochloric acid to produce a yellow solid precipitate that isolated by filtration, washed three times with distilled water (20 mL) and dried at 100 °C under vacuum. The solid compound was purified by column chromatographic technique, with petroleum ether/EtOAc (3:1) as eluents to finally yield the desired 3,6-dinitro-*9H*-carbazole ($Cz\text{-}2NO_2$) as yellow solid 5.16 g (85 %). mp: 244-245 °C. FT-IR (powder): 3400, 3091, 1611, 1583, 1519, 1484, 1339, 1310, 1245, 1098, 898, 812. ^{1}H NMR (DMSO-d_6, 25 °C, 500 MHz): δ = 12.69 (s, 1H), 9.48 (d, *J* = 3.0 Hz, 2H), 8.39 (dd, *J* = 9.0, 3.0 Hz, 2H), 7.76 (d, *J* = 9.0 Hz, 2H). ^{13}C NMR (DMSO-d_6, 25 °C, 125 MHz): δ = 161.67, 144.94, 127.13, 120.48, 119.49, 117.21, 114.92, 112.64.

Synthesis of 3,6-dinitro-9-(4-nitrophenyl)carbazole ($Cz\text{-}3NO_2$) [Scheme 1(a) and Scheme S1]

In a 100 mL two necked bottle, a mixture of 3,6-dinitro-9*H*-carbazole (2 g, 7.77 mmol) and potassium carbonate (5.37 g, 38.85 mmol) in dry DMSO (40 mL) was stirred for 10 min. under N_2 atmosphere. Then, 1-fluoro-4-nitrobenzene (1.65 mL, 15.55 mmol) was added gradually with continuous stirring, and the reaction mixture was allowed to heat under reflux at 140 °C for a period of 24 h. After cooling to ambient temperature and pouring slowly into distilled water (100 mL), a precipitate was formed. The obtained solid product was collected by filtration, washed thoroughly with distilled water (50 mL), and dried in oven under vacuum to give 3,6-dinitro-9-(4-nitrophenyl) carbazole as a brown solid 2.35 g (80%), m.p: > 300 °C. FT-IR (powder): 3084, 1611, 1591, 1587, 1510, 1335, 1300, 1273, 1231, 1170, 1104, 854, 839. ^{1}H NMR (DMSO-d_6, 25 °C, 500 MHz): δ = 9.30 (s, 1H), 9.07 (s, 1H), 8.83 (d, *J* = 7.8 Hz, 1H), 8.49 (d, *J* = 4.8 Hz, 2H), 8.13 (d, *J* = 9.6 Hz, 1H), 7.93 (d, *J* = 7.8 Hz, 1H), 7.91(d, *J* = 9.6 Hz, 1H), 7.75(d, *J* = 4.8 Hz, 2H). ^{13}C NMR (DMSO-d_6, 25 °C, 125 MHz): δ = 161.67, 144.94, 127.13, 120.48, 119.49, 117.21, 114.92, 112.64. MS (*m/e*): (378, 11%; 381, 100%).

Synthesis of 3,7-dinitro-10-(4-nitrophenyl)-10H-phenothiazine ($Tz\text{-}3NO_2$) [Scheme 1(b) and Scheme S2]

In a 250 mL two neck flask, a mixture of *10H*-phenothiazine (6.0 g, 30 mmol), dichloromethane (30 mL) and acetic acid (12 mL) had sodium nitrite (6.02 g, 87 mmol), were stirred for 10 min. at room temperature. Additional AcOH (12 mL), DCM (30 mL) and $NaNO_2$ (6.02 g) were then added. A further (30 mL) of AcOH was added to try and break up the thick reaction mixture. Finally, the mixture was stirred for 3 h. to give 3,7-dinitro-*10H*-phenothiazine derivative. In a 100 mL two necked bottle, charge dinitrophenothiazine (2.0 g, 7 mmol), *p*-fluoronitrobenzene (1.5 mL, 14 mmol) and potassium carbonate (4.8 g, 35 mmol) in DMSO (50 mL). Heat the previous mixture with reflux at 120 °C under nitrogen atmosphere for 4 days to obtain the targeted compound. After cooling to room temperature, the solution was poured into distilled water (150 mL), a colored solid was precipitated. The formed solid was collected by filtration, washed with distilled water (50 mL), and dried in oven under vacuum to produce 3,7-dinitro-10-(4-nitrophenyl)-*10H*-phenothiazine as a red solid 2.36 g (83 %), m.p: > 300 °C. FT-IR (powder): 3075, 1606, 1588, 1525, 1337, 1292, 1129, 851. MS (*m/e*): (409, 13%).

Synthesis of Azo-Cz-CMP [Scheme 2(a) and Scheme S3]

In a 25 mL Pyrex tube, a suspension sodium borohydride (33 mg, 0.87 mmol) dissolved in DMF (5 mL) was gradually added to a solution of 3,6-dinitro-9-(4-nitrophenyl)-carbazole (110 mg, 0.29 mmol) dissolved in DMF (5 mL). The resulting mixture was then heated at 85 °C under atmospheric pressure for 8 hrs. After cooling to room temperature (25 °C), the produced precipitate was collected by filtration, and washed 3 times with ethanol and 3 times with THF till colorless solution. Finally, the yielded precipitate was dried at oven overnight under vacuum to afford an orange solid of Azo-Cz-CMP, yield (89 %).

Synthesis of Azo-Tz-CMP [Scheme 2(b) and Scheme S4]

In a 25 mL Pyrex tube, sodium borohydride (27.67 mg, 0.73 mmol) dissolved in DMF (5 mL) was gradually added to a solution of 3,7-dinitro-10-(4-nitrophenyl)-*10H*-phenothiazine (100 mg, 0.24 mmol) dissolved in DMF (5 mL). The resulting mixture was then heated at 85 °C under atmospheric pressure for 8 h. After cooling to room temperature (25°C), the produced precipitate was collected by filtration, and washed 3 times with ethanol and 3 times with THF till colorless solution. Finally, the yielded precipitate was dried at oven overnight under vacuum to afford a red solid of Azo-Tz-CMP, yield (80%).

Characterization

FTIR spectra were recorded using a Bruker Tensor 27 FTIR spectrophotometer and the conventional KBr plate method; 32 scans were collected at a resolution of 4 cm^{-1}. Solid state NMR spectra were measured using a Bruker Avance 400 NMR spectrometer and a Bruker magic-angle-spinning (MAS) probe, running 32,000 scans. Mass spectra were recorded using a Bruker Solarix spectrometer. TGA was carried out by the utilizing of a TA Q-50 apparatus under N_2 gas stream. The Pt cell was packed and sealed with the tested

samples and subjected to heat from 40 to 800 °C at a heating average of 20 °C min^{-1} under N_2 atmosphere at a stream average of 50 mL min^{-1}. Specific surface areas and porosimetry investigations of the synthesized samples (ca. 20–100 mg) were carried by the utilization of a Micromeritics ASAP 2020 Surface Area and Porosity technique. The gradual exposition of the tested samples to N_2 gas (up to ca. 1 atm), in a bath of liquid N_2 (77 K) led to the generation of adsorption-desorption isotherms. A JEOL JSM-7610F scanning electron microscope was used to afford SEM morphology by subjecting the samples to Pt sputtering for a period of 100 s before the final observation. A JEOL-2100 scanning electron microscope was used to accomplish TEM analysis, that operated at 200 kV.

Results and discussions

Porous organic polymers (POPs) containing azo functional group as a linker between monomers can be synthesized either by aromatic amines oxidation polymerization reactions [58] or homo coupling reductive polymerization of nitro aromatics [66, 67] in the presence of metal catalyst. Our objective was to obtain azo-connected polymers holding carbazole or phenothiazine moieties and thus we adapted a direct homo reductive coupling of 3,6-dinitro-9-(4-nitrophenyl)-*9H*-carbazole or 3,7-dinitro-10-(4-nitrophenyl)-*10H*-phenothiazine in DMF solvent in the presence of sodium borohydride $NaBH_4$, under mild conditions without need of transition metal catalysts (Scheme 2). These CMPs were yielded in excellent yields (≥ 80%) and were insoluble in various organic solvents such as DMF, THF, DCM, EtOH, MeOH, and acetone, indicating that their structure possesses hyper cross-linked networks. In addition, they have a chemical stability upon treatment with strong acids (4M HCl) and bases (4M NaOH). The chemical structure of the studied monomers and CMPs were characterized using FTIR, solid state ^{13}C NMR and mass spectra. The starting monomer 3,6-dinitro-9-(4-nitrophenyl)-carbazole (Cz-$3NO_2$) has prepared as our reported publication (Figs. 1a and S1) [68]. The second monomer 3,7-dinitro-10-(4-nitrophenyl)-*10H*-phenothiazine (Tz-$3NO_2$) has synthesized by the stirring of a mixture of *10H*-phenothiazine and sodium nitrite in the presence of both dichloromethane and acetic acid to afford 3,7-dinitro-*10H*-phenothiazine derivative (Tz-$2NO_2$), which further refluxed under nitrogen atmosphere for 4 days with *p*-fluoronitrobenzene and potassium carbonate in DMSO to yield the target material (Tz-$3NO_2$) in high yield. FTIR spectra showed the existence of absorption bands at 1525, 1337 cm^{-1} which attributed to the symmetric and asymmetric stretching vibrations of N-O bond respectively, as well as a band at 3075 cm^{-1} characteristic of C-H aromatic stretching bond (Figs. 1c and S2). Mass spectroscopy represented a molecular ion peak at 409 m/z which is about 13 % of the base peak at 397 m/z. The formation of the azo bond in the synthesized CMPs was elucidated by the presence of new absorption bands at 1470 cm^{-1} and 1462 cm^{-1} in FTIR spectra of Azo-Cz and Azo-Tz, respectively, attributed to

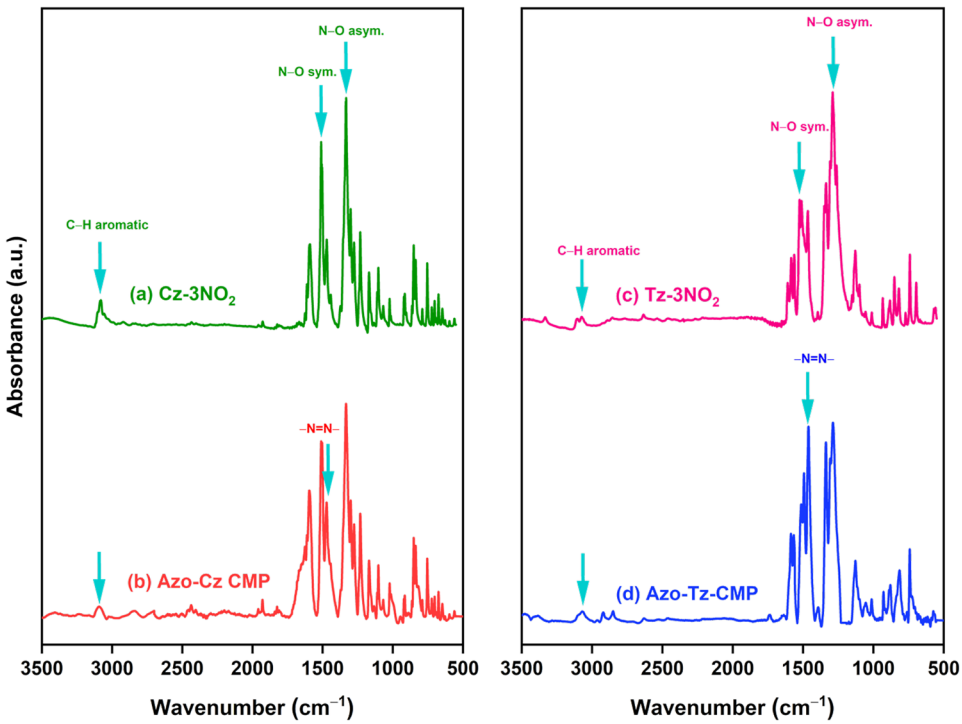

Fig. 1 FTIR spectroscopy of (**a**) Cz-$3NO_2$, (**b**) Azo-Cz-CMP, (**c**) Tz-$3NO_2$ and (**d**) Azo-Tz-CMP

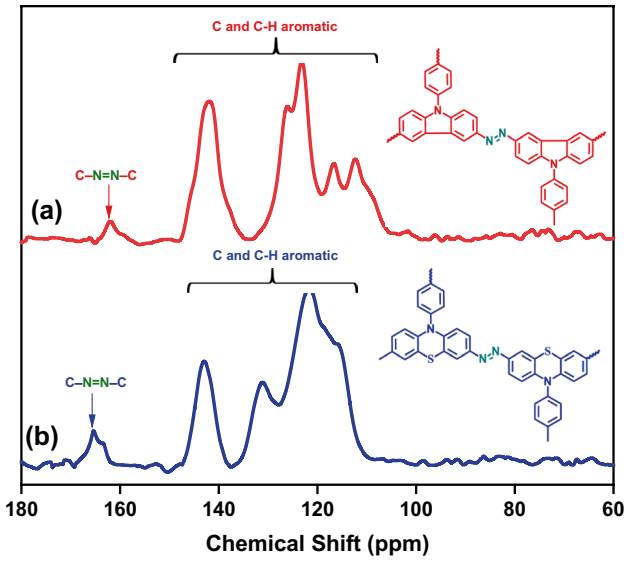

Fig. 2 Solid state ^{13}C NMR spectra of (**a**) Azo-Cz-CMP and (**b**) Azo-Tz-CMP

asymmetric vibration of the N=N bond (Fig. 1b, d). Also, the IR spectra of CMPs displayed the disappearance of absorption bands at 1510 cm^{-1}, and 1525 cm^{-1} for N-O symmetric stretching vibrations of Cz-3NO_2 and Tz-3NO_2, respectively, as well as vanishing two bands at 1332 cm^{-1}, and 1337 cm^{-1} for N-O asymmetric stretching vibrations of Cz-3NO_2 and Tz-3NO_2, respectively, along with bands for aromatic rings at 3080 and 3071 cm^{-1} for Azo-Cz and Azo-Tz, suggesting successful polymerization reaction (Figs. 1b, d, and S3, S4). Furthermore, the formation of azo-bridged functional group was more proved by the existence of a signal at ca. 162 and 165 ppm that assigned to -C-N=N-C- linkage in solid state ^{13}C NMR spectra of Azo-Cz and Azo-Tz-CMPs, respectively, in addition to other signals corresponding to the remaining aromatic carbons (150-110 ppm) in their skeletons as shown in (Fig. 2a, b).

Thermal stability of these azo-linked CMPs was investigated by TGA (thermal gravimetric analysis). Measuring was carried out in a nitrogen atmosphere at heating average of 10 °C/min reaching to 800 °C. Thermal degradation temperature (T_d = 10 % weight loss) were confirmed to be 383 °C, and 386 °C corresponding to Azo-Cz and Azo-Tz CMPs, respectively, which imply a significant thermal stability. Char yields of these obtained CMPs had intermediate values up to 41 % and 46 % for Azo-Cz and Azo-Tz CMPs, respectively as shown in Fig. 3a, b and Table 1. The porosity of azo-bridged polymers was characterized by the utilization of nitrogen sorption isotherms measured at 77 K. Azo-Cz-CMP showed a combination of type-II sorption behaviors (Fig. 4a, c) according to the IUPAC ranking. Nitrogen gas adsorption was very rapidly at low relative pressure (P/P_0), which prove the microporous feature of the Azo-Cz-CMP network. Reaching to the high pressure region, there is a directly proportional between the nitrogen sorption with increasing

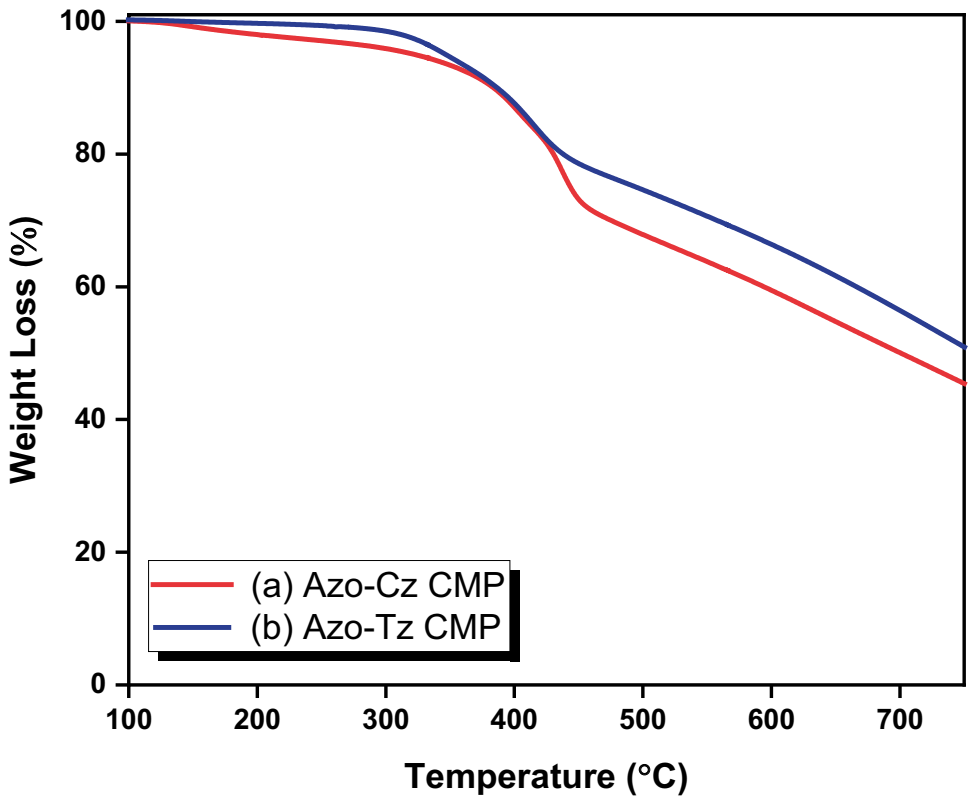

Fig. 3 TGA curves of (**a**) Azo-Cz-CMP and (**b**) Azo-Tz-CMP

Table 1 Thermal stability and porosity properties of Azo-Cz-CMP and Azo-Tz-CMP

Sample	T_{d5} (°C)	T_{d10} (°C)	Char yield (wt%)	Surface area ($m^2\ g^{-1}$)	Pore size (nm)
Azo-Cz-CMP	322	383	41	315	0.79
Azo-Tz-CMP	346	386	46	225	1.18

relative pressure. Azo-Cz-CMP represented the BET surface area up to 315 $m^2\ g^{-1}$, with total pore volume of 0.05 $cm^3\ g^{-1}$, and the pore size centered at 0.79 nm, as obtained by the nonlocal density functional theory (NLDFT). However, Azo-Tz-CMP displayed the lower BET surface area of 225 $m^2\ g^{-1}$, the total pore volume reaching 0.12 $cm^3\ g^{-1}$, and the pore size mainly centered at 1.18 nm as well (Fig. 4b, d). The porosity properties of these two Azo-CMPs were also summarized in Table 1. The obtained results based on FTIR, solid state NMR, TGA and BET analyses were all confirmed the successful preparation of these two azo-based CMPs in this study. The morphology of these studied azo-based CMPs was monitored using both FE-SEM and TEM analyses, which indicate the presence of irregular shapes with nanoscale aggregates based on SEM images (Fig. 5a, b). While, TEM images showed that these azo-based CMPs had microporous structures as shown in Fig. 5c−f, which is consistent with BET analyses.

Porous materials have N atoms within their structures display an excellent potency to interact with CO_2 molecules, resulting in enhancing the CO_2 uptake. Our synthesized azo-based CMPs have a good nitrogen contents and good surface areas that enabled them to be tested for their suitability

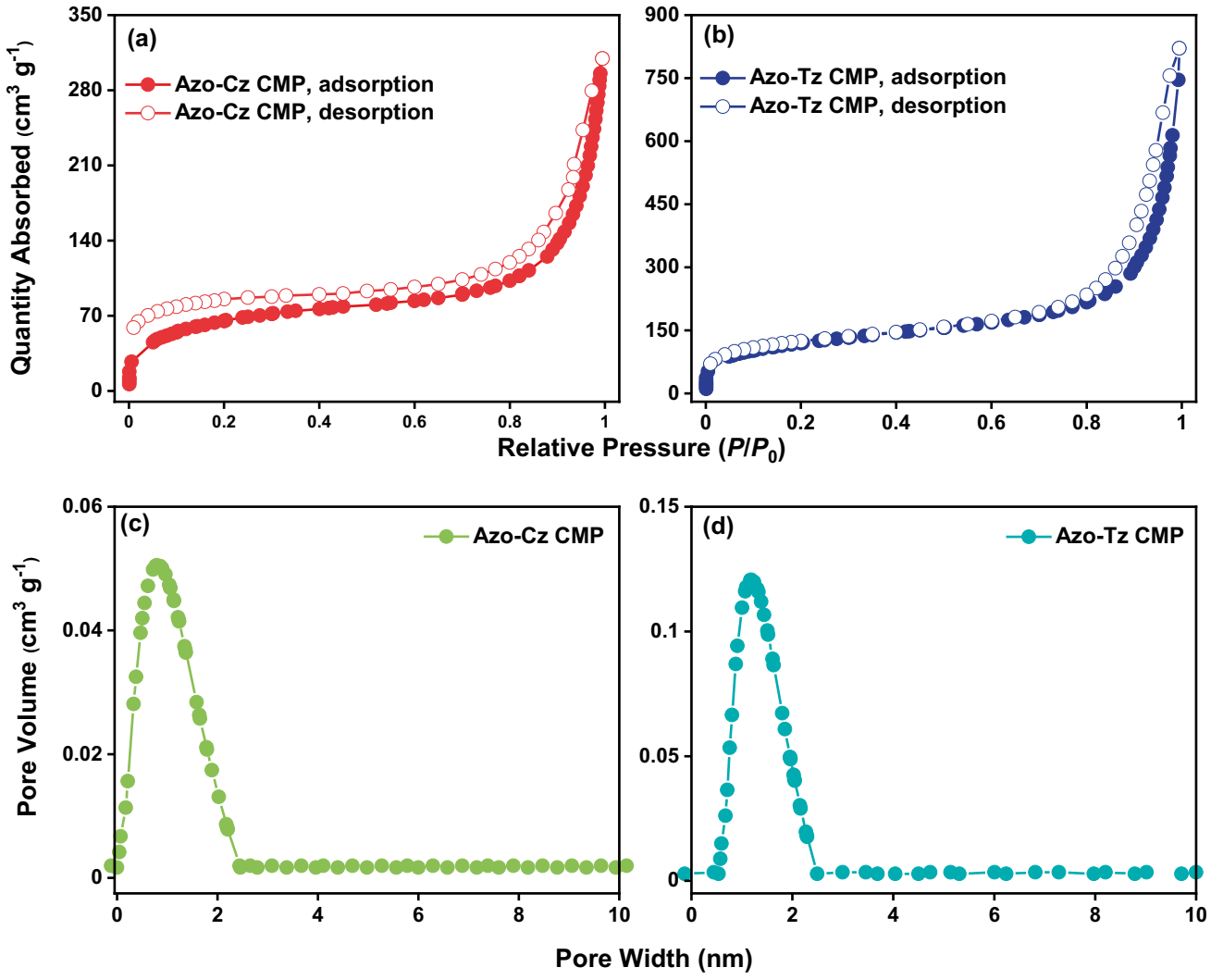

Fig. 4 Nitrogen adsorption/desorption isotherms of (**a**) Azo-Cz-CMP and (**b**) Azo-Tz-CMP. As well as curves of pore size distribution of (**c**) Azo-Cz-CMP and (**d**) Azo-Tz-CMP

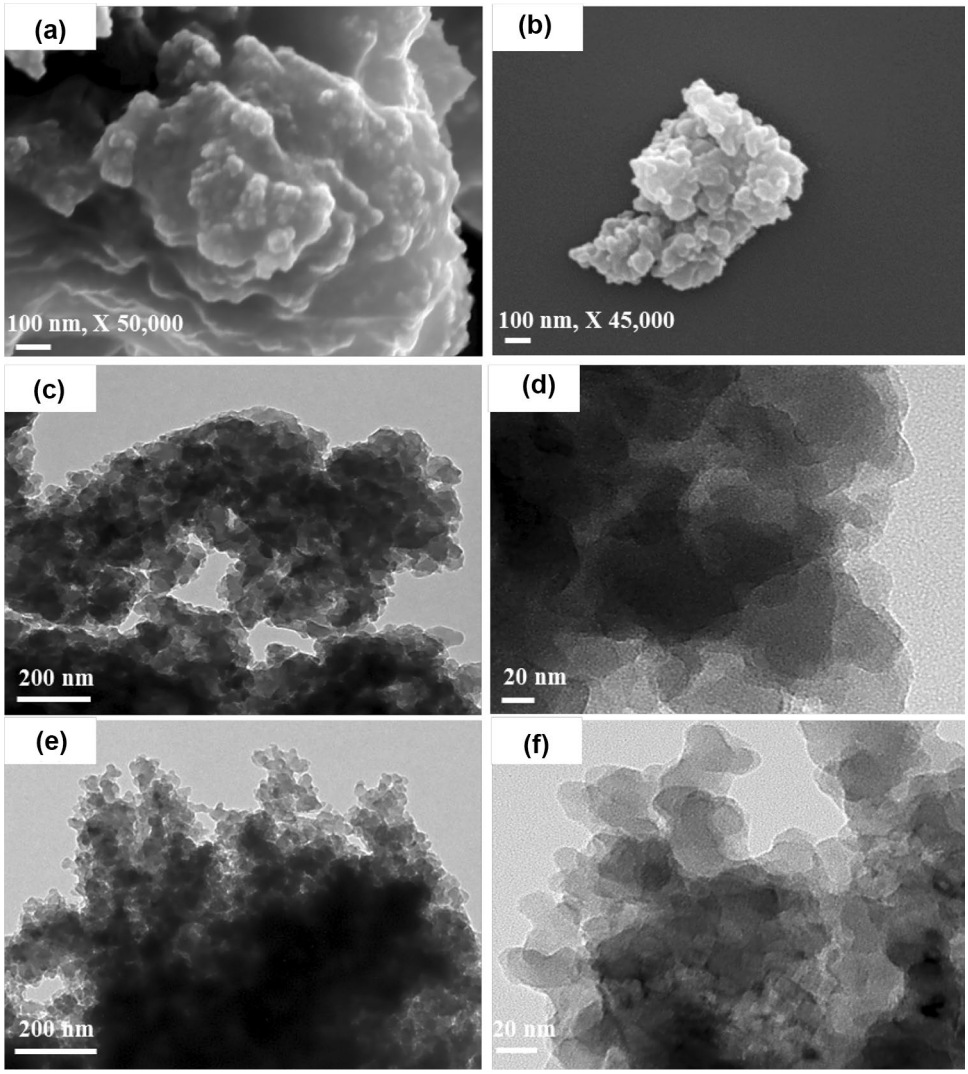

Fig. 5 SEM photos of (**a**) Azo-Cz-CMP, (**b**) Azo-Tz-CMP. TEM images of (**c**, **d**) Azo-Cz-CMP, (**e**, **f**) Azo-Tz-CMP

in CO_2 capture application. The prepared azo-based CMPs have been examined for the CO_2 adsorption capacities at temperatures of 298 K and 273 K and pressure reaching to 1 bar as shown in Fig. 6a, b. From the obtained results, one can conclude that the Azo-Cz-CMP had the top CO_2 capture values: 40 and 94 mg g^{-1} at the experiment temperatures 298 K and 273 K, respectively. On the other side, the Azo-Tz-CMP presented the lowest CO_2 values of 28 and 60 mg g^{-1} at the same corresponding temperatures. The higher CO_2 uptake efficiencies of the Azo-Cz-CMP compared to the Azo-Tz-CMP, was mainly attributed to its high surface area and large pore volumes that consume more CO_2 molecules. Noticeably, the CO_2 uptake efficacy of our tested CMPs are among the highest reported Azo-linked CMPs [69–71]. In addition, they represented a significant CO_2 adsorption capacity relative to other porous substances [27, 68, 72]. Moreover, the isosteric heats of adsorption (Q_{st}) of these azo-based CMPs were calculated from their CO_2 adsorption at 298 K and 273 K, by the aid of Clausius–Clapeyron equation as shown in Fig. 7a, b. The Azo-Cz-CMP provided good values of Q_{st} up to 32.08 and 23.69 kJ mol^{-1} at the minimum and maximum values of CO_2 uptake (ca. 0.1 and 0.8 mmol g^{-1}), respectively. Whereas, the other Azo-Tz-CMP showed calculated values of Q_{st} at low and high adsorptions of CO_2 (ca. 0.1 and 0.8 mmol g^{-1}) of 18.36 and 10.90 kJ mol^{-1}, respectively. The observed values of Q_{st} confirm our suggestion of the strong interaction between our CMPs and CO_2 molecules, similar to the behavior of activated carbons (Table 2) [73].

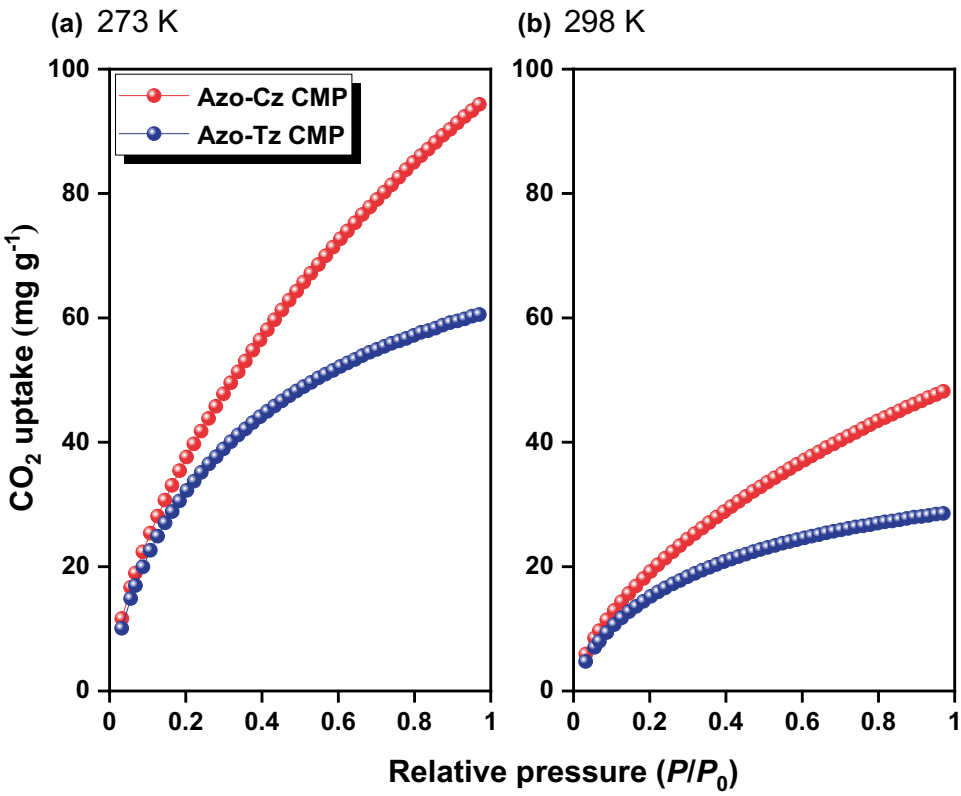

Fig. 6 CO_2 uptake curves of (**a**) the Azo-Cz-CMP and the Azo-Tz-CMP measured at 273 K. (**b**) the Azo-Cz-CMP and the Azo-Tz-CMP measured at 298 K

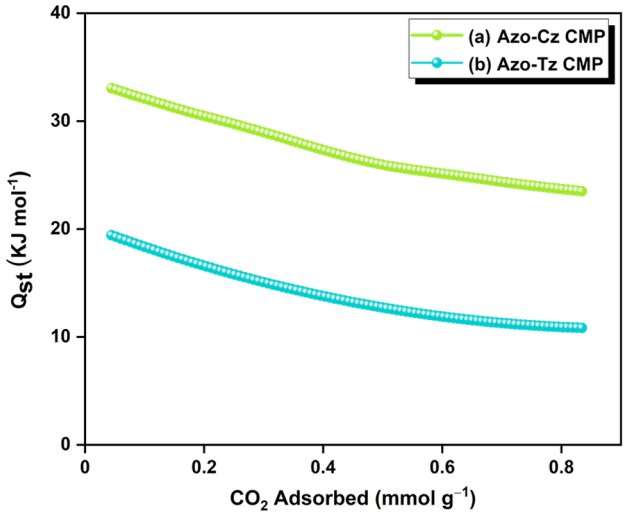

Fig. 7 Isosteric heat of adsorption (Qst) for (**a**) Azo-Cz-CMP and (**b**) Azo-Tz-CMP obtained from the CO_2 uptake isotherms collected at 298 and 273 K

Table 2 Adsorption capacity values of CO_2 in the pores of Azo-Cz-CMP, and Azo-Tz-CMP, comparable with those of other reported adsorbents

Adsorbent	CO_2 uptake (mg g^{-1}) 273 K	CO_2 uptake (mg g^{-1}) 298 K	Ref.
Azo-POF-2	84.5	55.1	61
Ene-POF-1	86.4	50.0	61
Ene-POF-2	70.7	40.2	61
Azo-CPP-4	94.3	----	62
Azo-CPP-5	94.3	----	62
Azo-CPP-6	81.5	----	62
Azo-CPP-7	82.9	----	62
Azo-MOP-3	81.2	----	63
Azo-MOP-4	77.7	----	63
Azo-MOP-1-Ru	59.5	----	63
Azo-MOP-3-Ru	82.1	----	63
Azo-MOP-4-Ru	52.8	----	63
TPA-COF-3	91.1	63.9	22
TPA-COF-2	82.4	45.9	22
TPT-COF-5	59.4	41	22
Car-TPP-COF	62	34	60
Car-TPT-COF	73	42	60
Mesoporous silica	90.2	----	64
Azo-Cz-CMP	94	40	**This work**
Azo-Tz-CMP	60	28	**This work**

Conclusions

In this presented study, we reported the design and synthesis of two novel azo-linked conjugated microporous polymers (Azo-Cz-CMP and Azo-Tz-CMP) via the reductive coupling of the corresponding nitro monomers. FTIR and solid state NMR spectroscopy were used to confirm their chemical structures. The Azo-Cz-CMP possessed good BET specific surface area up to 315 $m^2\ g^{-1}$ and a considerable thermal stability. Our CMPs were tested for their suitability for CO_2 uptake as an environmental application. The Azo-Cz-CMP provided a very good CO_2 adsorption efficiency up to 40 and 94 mg g^{-1} at 298 and 273 K, respectively, owing to its reasonable surface area, suitable pore volumes, and good Q_{st} value for CO_2. The presence of N atoms within the chemical structures of the resultant CMPs encouraged the considerable quadrupolar interactions with CO_2 molecules. On account of their high gas uptake efficacies, and good physicochemical stability, the studied CMPs considered among the most promised candidates for small gas storage and separation applications.

Supplementary information The online version contains supplementary material available at https://doi.org/10.1007/s10965-021-02803-8.

Acknowledgements This study was supported financially by Ministry of Science and Technology, Taiwan, under contracts MOST 108-2218-E-110-013-MY3 and MOST 110-2636-E-007-020.

Declarations

Conflict of interest The authors declare no conflict of interest

References

1. Figueroa JD, Fout T, Plasynski S, McIlvried H, Srivastava RD (2008) Advances in CO_2 Capture Technology—The U.S. Department of Energy's Carbon Sequestration Program. Int J Greenhouse Gas Control 2:9–20. https://doi.org/10.1016/S1750-5836(07)00094-1
2. Doney SC, Fabry VJ, Feely RA, Kleypas JA (2009) Ocean Acidification: The Other CO_2 Problem. Annu Rev Mar Sci 1:169–192. https://doi.org/10.1146/annurev.marine.010908.163834
3. Oppenheimer M, Alley RB (2004) The West Antarctic Ice Sheet and Long Term Climate Policy. Clim Change 64:1–10. https://doi.org/10.1023/B:CLIM.0000024792.06802.31
4. Sevilla M, Fuertes AB (2011) Sustainable porous carbons with a superior performance for CO_2 capture. Energy Environ Sci 4:1765–1771. https://doi.org/10.1039/C0EE00784F
5. BP (2015) Statistical Review of World Energy June 2015. London
6. Rackley SA (2009) Carbon Capture and Storage, Butter worth Heinemann: Oxford, U.K
7. Le Qu´er´e C, Jackson RB, Jones MW, Smith AJ, Abernethy S, Andrew RM, De-Gol AJ, Willis DR, Shan Y, Canadell JG, Friedlingstein P, Creutzig F, Peters GP (2020) Temporary reduction in daily global CO_2 emissions during the COVID-19 forced confinement. Nat Clim Change 10:647–653. https://doi.org/10.1038/s41558-020-0797-x
8. Li F, Fan LS (2008) Clean coal conversion processes – progress and challenges. Energy Environ Sci 1:248–267. https://doi.org/10.1039/B809218B
9. Zeng Y, Zou R, Zhao Y (2016) Covalent organic frameworks for CO_2 capture. Adv Mater 28:2855–2873. https://doi.org/10.1002/adma.201505004
10. Merkel TC, Lin H, Wei X, Baker R (2010) Power plant post combustion carbon dioxide capture: an opportunity for membranes. J Membr Sci 359:126–139. https://doi.org/10.1016/j.memsci.2009.10.041
11. Sang YF, Chen G, Huang JG (2020) Oxygen-rich porous carbons from carbonyl modified hyper-cross-linked polymers for efficient CO_2 capture. J Polym Res 27:36. https://doi.org/10.1007/s10965-020-2009-9
12. An J, Geib SJ, Rosi NL (2010) High and selective CO_2 uptake in a cobalt adeninate metal-organic framework exhibiting pyrimidine- and amino-decorated pores. J Am Chem Soc 132:38–39. https://doi.org/10.1021/ja909169x
13. Zhang X, Lu J, Zhang J (2014) Porosity Enhancement of Carbazolic Porous Organic Frameworks Using Dendritic Building Blocks for Gas Storage and Separation. Chem Mater 26:4023–4029. https://doi.org/10.1021/cm501717c
14. Liu Y, Zhang J, Huang H, Huang Z, Xu C, Guo G, He H, Ma J (2019) Treatment of trace thallium in contaminated source waters by ferrate pre-oxidation and poly aluminium chloride coagulation. Sep Purif Technol 227:115663. https://doi.org/10.1016/j.seppur.2019.06.001
15. Hsiao CY, Hung C, Kwon E, Huang CW, Huang CF, Lin KYA (2021) Electrospun nanoscale iron oxide-decorated carbon fiber as an efficient heterogeneous catalyst for activating percarbonate to degrade Azorubin S in water. J Water Process Eng 40:101838. https://doi.org/10.1016/j.jwpe.2020.101838
16. Ding M, Flaig RW, Jiang HL, Yaghi OM (2019) Carbon capture and conversion using metal– organic frameworks and MOF-based materials. Chem Soc Rev 48:2783–2828. https://doi.org/10.1039/C8CS00829A
17. EL-Mahdy AFM, Yu TC, Kuo SW (2021) Synthesis of multiple heteroatom–doped mesoporous carbon/silica composites for supercapacitors. Chem Eng J 414:128796. https://doi.org/10.1016/j.cej.2021.128796
18. Abuzeid HR, EL-Mahdy AFM, Kuo SW (2020) Hydrogen bonding induces dual porous types with microporous and mesoporous covalent organic frameworks based on bicarbazole units. Micropor Mesopor Mat 300:110151. https://doi.org/10.1016/j.micromeso.2020.110151
19. Abuzeid HR, EL-Mahdy AFM, Kuo SW (2021) Covalent organic frameworks: design principles, synthetic strategies, and diverse applications. Giant 6:100054. https://doi.org/10.1016/j.giant.2021.100054
20. EL-Mahdy AFM, Yu TC, Mohamed MG, Kuo SW (2021) Secondary structures of polypeptide-based diblock copolymers influence the microphase separation of templates for the fabrication of microporous carbons. Macromolecules 54:1030–1042. https://doi.org/10.1021/acs.macromol.0c01748
21. Mohamed MG, Tsai MY, Su WC, EL-Mahdy AFM, Wang CF, Huang CF, Dai L, Chen T, Kuo SW (2020) Nitrogen-Doped microporous carbons derived from azobenzene and nitrile-functionalized polybenzoxazines for CO_2 uptake. Mater Today Commun 24:1011112. https://doi.org/10.1016/j.mtcomm.2020.101111
22. EL-Mahdy AFM, Liu TE, Kuo SW (2020) Direct synthesis of nitrogen-doped mesoporous carbons from triazine-functionalized resol for CO_2 uptake and highly efficient removal of dyes. J Hazard Mater 391:122163–122177. https://doi.org/10.1016/j.jhazmat.2020.122163
23. Ghalia MA, Dahman Y (2017) Development and evaluation of zeolites and metal–organic frameworks for carbon dioxide

separation and capture. Energy Technol 5:356–372. https://doi.org/10.1002/ente.201600359
24. EL-Mahdy AFM, Hung YH, Mansoure TH, Yu HH, Hsu YS, Wu KCW, Kuo SW (2019) Synthesis of [3 + 3] β-ketoenamine-tethered covalent organic frameworks (COFs) for high-performance supercapacitance and CO_2 storage. J Taiwan Inst Chem Eng 103:199–208. https://doi.org/10.1016/j.jtice.2019.07.016
25. EL-Mahdy AFM, Kuo CH, Alshehri A, Young C, Yamauchi Y, Kim J, Kuo SW (2018) Strategic design of triphenylamine- and triphenyltriazine-based two-dimensional covalent organic frameworks for CO_2 uptake and energy storage. J Mater Chem A 6:19532–19541. https://doi.org/10.1039/C8TA04781B
26. Mohamed MG, Ebrahium SM, Hamman AS, Kuo SW, Aly KI (2020) Enhanced CO_2 capture in nitrogen-enriched microporous carbons derived from Polybenzoxazines containing azobenzene and carboxylic acid units. J Polym Res 27:197. https://doi.org/10.1007/s10965-020-02179-1
27. Mohamed MG, EL-Mahdy AFM, Takashi Y, Kuo SW (2020) Ultrastable conductive microporous covalent triazine frameworks based on pyrene moieties provide high-performance CO_2 uptake and supercapacitance. New J Chem 44:8241–8253. https://doi.org/10.1039/D0NJ01292K
28. El-Mahdy AFM, Zakaria MB, Wang HX, Chen T, Yamauchi Y, Kuo SW (2020) Heteroporous bifluorenylidene-based covalent organic frameworks displaying exceptional dye adsorption behavior and high energy storage. J Mater Chem A 8:25148–25155. https://doi.org/10.1039/D0TA07281H
29. Ahmed LR, EL-Mahdy AFM, Pan CT, Kuo SW (2021) A water-soluble copper-immobilized covalent organic framework functioning as an OFF–ON fluorescent sensor for amino acids. Mater Adv 2:4617–4629. https://doi.org/10.1039/D1MA00234A
30. EL-Mahdy AFM, Lüder J, Kotp MG, Kuo SW (2021) A Tröger's base-derived covalent organic polymer containing carbazole units as a high-performance supercapacitor. Polymers 13(9):1385. https://doi.org/10.3390/polym13091385
31. Mohamed MG, Chen WC, EL-Mahdy AFM, Kuo SW (2021) Porous organic/inorganic polymers based on double-decker silsesquioxane for high-performance energy storage. J Polym Res 28:219. https://doi.org/10.1007/s10965-021-02579-x
32. Hussain MW, Bandyopadhyay S, Patra A (2017) Microporous organic polymers involving thiadiazolopyridine for high and selective uptake of greenhouse gases at low pressure. Chem Commun 53:10576–10579. https://doi.org/10.1039/C7CC05097F
33. Elewa AM, Elsayed MH, El-Mahdy AFM, Chang CL, Ting LY, Lin WC, Lu CY, Chou HH (2021) Triptycene-based discontinuously-conjugated covalent organic polymer photocatalysts for visible-light-driven hydrogen evolution from water. Appl Catal B-Environ 285:119802. https://doi.org/10.1016/j.apcatb.2020.119802
34. Wang S, Song K, Zhang C, Shu Y, Li T, Tan B (2017) A novel metalporphyrin-based microporous organic polymer with high CO_2 uptake and efficient chemical conversion of CO_2 under ambient conditions. J Mater Chem A 5:1509–1515. https://doi.org/10.1039/C6TA08556C
35. Mohamed MG, Zhang X, Mansoure TH, EL-Mahdy AFM, Huang CF, Danko M, Xin Z, Kuo SW (2020) Hypercrosslinked porous organic polymers based on tetraphenylanthraquinone for CO_2 uptake and high-performance supercapacitor. Polymer 205:122857–122867. https://doi.org/10.1016/j.polymer.2020.122857
36. Gu S, He J, Zhu Y, Wang Z, Chen D, Yu G, Pan C, Guan J, Tao K (2016) Facile carbonization of microporous organic polymers into hierarchically porous carbons targeted for effective CO_2 uptake at low pressures. ACS Appl Mater Interfaces 8:18383–18392. https://doi.org/10.1021/acsami.6b05170
37. Elewa AM, EL-Mahdy AFM, Elsayed MH, Mohamed MG, Kuo SW, Chou HH (2021) Sulfur-doped triazine-conjugated microporous polymers for achieving the robust visible-light-driven hydrogen evolution. Chem Eng J 421:129825. https://doi.org/10.1016/j.cej.2021.129825
38. EL-Mahdy AFM, Elewa AM, Huang SW, Chou HH, Kuo SW (2020) Dual-Function Fluorescent Covalent Organic Frameworks: HCl Sensing and Photocatalytic H_2 Evolution from Water. Adv Optical Mater 8:2000641. https://doi.org/10.1002/adom.202000641
39. Rouquerol J, Avnir D, Fairbridge CW, Everett DH, Haynes JH, Pernicone N, Ramsay JDF, Sing KSW, Unger KK (1994) Recommendations for the Characterization of Porous Solids. Pure Appl Chem 66:1739–1758. https://doi.org/10.1351/pac199466081739
40. Xu Y, Jin S, Xu H, Nagai A, Jiang D (2013) Conjugated microporous polymers: design, synthesis and application. Chem Soc Rev 42:8012–8031. https://doi.org/10.1039/C3CS60160A
41. Cooper AI (2009) Conjugated Microporous Polymers. Adv Mater 21:1291–1295. https://doi.org/10.1002/adma.200801971
42. Wu D, Xu F, Sun B, Fu R, He H, Matyjaszewski K (2012) Design and Preparation of Porous Polymers. Chem Rev 112:3959–4015. https://doi.org/10.1021/cr200440z
43. Dawson R, Cooper AI, Dams DJ (2012) Nanoporous organic polymer networks. Prog Polym Sci 37:530–563. https://doi.org/10.1016/j.progpolymsci.2011.09.002
44. Ma BC, Ghasimi S, Landfester K, Vilela F, Zhang KAI (2015) Conjugated microporous polymer nanoparticles with enhanced dispersibility and water compatibility for photocatalytic applications. J Mater Chem A 3:16064–16071. https://doi.org/10.1039/C5TA03820K
45. Wood CD, Tan B, Trewin A, Niu HJ, Bradshaw D, Rosseinsky MJ, Khimyak YZ, Campbell NL, Kirk R, Stockel E, Cooper AI (2007) Hydrogen Storage in Microporous Hypercrosslinked Organic Polymer Networks. Chem Mater 19:2034–2048. https://doi.org/10.1021/cm070356a
46. Dawson R, Adams DJ, Cooper AI (2011) Chemical tuning of CO_2 sorption in robust nanoporous organic polymers. Chem Sci 2:1173–1177. https://doi.org/10.1039/C1SC00100K
47. Kou Y, Xu YH, Guo ZQ, Jiang D (2011) Supercapacitive energy storage and electric power supply using an aza-fused pi-conjugated microporous framework. Angew Chem Int Ed 50:8753–8757. https://doi.org/10.1002/anie.201103493
48. Zhuang X, Zhang F, Wu D, Forler N, Liang H, Wagner M, Gehrig D, Hansen MR, Feng Laquai FX (2013) Two-Dimensional Sandwich-Type, Graphene-Based Conjugated Microporous Polymers. Angew Chem Int Ed 52:9668–9672. https://doi.org/10.1002/anie.201304496
49. Xu Y, Nagai YA, Jiang D (2013) Core–shell conjugated microporous polymers: a new strategy for exploring color-tunable and -controllable light emissions. Chem Commun 49:1591–1593. https://doi.org/10.1039/C2CC38211C
50. Xu Y, Chen L, Guo Z, Nagai A, Jiang D (2011) Light-Emitting Conjugated Polymers with Microporous Network Architecture: Interweaving Scaffold Promotes Electronic Conjugation, Facilitates Exciton Migration, and Improves Luminescence. J Am Chem Soc 133:17622–17625. https://doi.org/10.1021/ja208284t
51. Chen Q, Wang JX, Yang F, Zhou D, Bian N, Zhang XJ, Yan CG, Han BH (2011) Tetraphenylethylene-based fluorescent porous organic polymers: preparation, gas sorption properties and photoluminescence properties. J Mater Chem 21:13554–13560. https://doi.org/10.1039/C1JM11787D
52. Rao KV, Mohapatra S, Maji TK, George SJ (2012) Guest-Responsive Reversible Swelling and Enhanced Fluorescence in a Super-Absorbent, Dynamic Microporous Polymer. Chem A Eur J 18:4505–4509. https://doi.org/10.1002/chem.201103750

53. Zhang K, Kopetzki D, Seeberger PH, Antonietti M, Vilela F (2013) Surface Area Control and Photocatalytic Activity of Conjugated Microporous Poly(benzothiadiazole) Networks. Angew Chem Int Ed 52:1432–1436. https://doi.org/10.1002/anie.201207163
54. Cao Q, Yin Q, Chen Q, Dong ZB, Han BH (2017) Fluorinated Porous Conjugated Polyporphyrins through Direct C−H Arylation Polycondensation: Preparation, Porosity, and Use as Heterogeneous Catalysts for Baeyer-Villiger Oxidation. Chem A Eur J 23:9831–9837. https://doi.org/10.1002/chem.201700916
55. Yan Z, Yuan Y, Tian Y, Zhang D, Zhu G (2015) Highly Efficient Enrichment of Volatile Iodine by Charged Porous Aromatic Frameworks with Three Sorption Sites. Angew Chem Int Ed 54:12733–12737. https://doi.org/10.1002/anie.201503362
56. Katsoulidis AP, Kanatzidis MG (2011) Phloroglucinol Based Microporous Polymeric Organic Frameworks with - OH Functional Groups and High CO_2 Capture Capacity. Chem Mater 23:1818–1824. https://doi.org/10.1021/cm103206x
57. Deria P, Mondloch JE, Tylianakis E, Ghosh P, Bury W, Snurr RQ, Hupp JT, Farha OK (2013) Perfluoroalkane Functionalization of NU-1000 via Solvent-Assisted Ligand Incorporation: Synthesis and CO_2 Adsorption Studies. J Am Chem Soc 135:16801–16804. https://doi.org/10.1021/ja408959g
58. Konstas KJ, Taylor W, Thornton AW, Doherty CM, Lim WX, Bastow TJ, Kennedy DF, Wood CD, Cox BJ, Hill JM, Hill AJ, Hill MR (2012) Lithiated porous aromatic frameworks with exceptional gas storage capacity. Angew Chem Int Ed 51:6639–6642. https://doi.org/10.1002/anie.201201381
59. Zhao H, Jin Z, Su H, Zhang J, Yao X, Zhao H, Zhu G (2013) Target synthesis of a novel porous aromatic framework and its highly selective separation of CO_2/CH_4. Chem Commun 49:2780–2782. https://doi.org/10.1039/C3CC38474H
60. Xu C, Hedin N (2013) Synthesis of microporous organic polymers with high CO_2-over-N_2 selectivity and CO_2 adsorption. J Mater Chem A 1:3406–3414. https://doi.org/10.1039/C3TA01160G
61. Gomes R, Bhaumik A (2016) A new triazine functionalized luminescent covalent organic framework for nitroaromatic sensing and CO_2 storag. RSC Adv 6:28047–28054. https://doi.org/10.1039/C6RA01717G
62. Yu H, Tian M, Shen C, Wang Z (2013) Facile preparation of porous polybenzimidazole networks and adsorption behavior of CO_2 gas, organic and water vapor. Polym Chem 4:961–968. https://doi.org/10.1039/C2PY20908J
63. Islamoğlu T, Rabbani MG, El-Kaderi HM (2013) Impact of post-synthesis modification of nanoporous organic frameworks on small gas uptake and selective CO_2 capture. J Mater Chem A 1:10259–10266. https://doi.org/10.1039/C3TA12305G
64. Arab P, Parrish E, Islamoglu T, El-Kaderi HM (2015) Synthesis and evaluation of porous azo-linked polymers for carbon dioxide capture and separation. J Mater Chem A 3:20586–20594. https://doi.org/10.1039/C5TA04308E
65. Arab P, Rabbani MG, Sekizkardes AK, Islamo˘glu T, El-Kaderi HM (2014) Copper(I)-Catalyzed Synthesis of Nanoporous Azo-Linked Polymers: Impact of Textural Properties on Gas Storage and Selective Carbon Dioxide Capture. Chem Mater 26:1385–1392. https://doi.org/10.1021/cm403161e
66. Dang QQ, Wang XM, Zhan YF, Zhang XM (2016) An azo-linked porous triptycene network as an absorbent for CO_2 and iodine uptake. Polym Chem 7:643–647. https://doi.org/10.1039/C5PY01671A
67. Lu J, Zhang J (2014) Facile synthesis of azo-linked porous organic frameworks via reductive homo coupling for selective CO_2 capture. J Mater Chem A 2:13831–13834. https://doi.org/10.1039/C4TA03015J
68. El-Mahdy AFM, Young C, Kim J, You J, Yamauchi Y, Kuo SW (2019) Hollow microspherical and microtubular [3+3] carbazole-based covalent organic frameworks and their gas and energy storage applications. ACS Appl Mater Interfaces 11:9343–9354. https://doi.org/10.1021/acsami.8b21867
69. Lu J, Zhang J (2014) Facile synthesis of azo-linked porous organic frameworks via reductive homocoupling for selective CO_2 capture. J Mater Chem A 2:13831–13834. https://doi.org/10.1039/C4TA03015J
70. Tao L, Niu F, Zhang D, Liu J, Wanga T, Wang Q (2015) Azo-bridged covalent porphyrinic polymers (AzoCPPs): synthesis and CO_2 capture properties. RSC Adv 5:96871–96878. https://doi.org/10.1039/C5RA17671A
71. Yang Z, Zhang H, Yu B, Zhao Y, Ma Z, Ji G, Han B, Liu Z (2015) Azo-functionalized microporous organic polymers: Synthesis and applications in CO_2 capture and conversion. ChemComm 51:11576–11579. https://doi.org/10.1039/C5CC03151F
72. Serna-Guerrero R, Belmabkhout Y, Sayari A (2010) Further investigations of CO_2 capture using triamine-grafted pore-expanded mesoporous silica. Chem Eng J 158:513–519. https://doi.org/10.1016/j.cej.2010.01.041
73. Keskin S, van Heest TM, Sholl DS (2010) Can metal–organic framework materials play a useful role in large-scale carbon dioxide separations. Chem Sus Chem 3:879–891. https://doi.org/10.1002/cssc.201000114